On the excited electronic state dissociation of nitramine energetic materials and model systems

Y. Q. Guo, M. Greenfield, A. Bhattacharya, and E. R. Bernstein

Citation: The Journal of Chemical Physics **127**, 154301 (2007); doi: 10.1063/1.2787587
View online: http://dx.doi.org/10.1063/1.2787587
View Table of Contents: http://aip.scitation.org/toc/jcp/127/15
Published by the American Institute of Physics

THE JOURNAL OF CHEMICAL PHYSICS **127**, 154301 (2007)

On the excited electronic state dissociation of nitramine energetic materials and model systems

Y. Q. Guo, M. Greenfield, A. Bhattacharya, and E. R. Bernstein[a]
Department of Chemistry, Colorado State University, Fort Collins, Colorado 80523-1872, USA

(Received 16 April 2007; accepted 29 August 2007; published online 15 October 2007)

In order to elucidate the difference between nitramine energetic materials, such as RDX (1,3,5-trinitro-1,3,5-triazacyclohexane), HMX (1,3,5,7-tetranitro-1,3,5,7-tetraazacyclooctane), and CL-20 (2,4,6,8,10,12-hexanitro-2,4,6,8,10,12-hexaazaisowurtzitane), and their nonenergetic model systems, including 1,4-dinitropiperazine, nitropiperidine, nitropyrrolidine, and dimethylnitramine, both nanosecond mass resolved excitation spectroscopy and femtosecond pump-probe spectroscopy in the UV spectral region have been employed to investigate the mechanisms and dynamics of the excited electronic state photodissociation of these materials. The NO molecule is an initial decomposition product of all systems. The NO molecule from the decomposition of energetic materials displays cold rotational and hot vibrational spectral structures. Conversely, the NO molecule from the decomposition of model systems shows relatively hot rotational and cold vibrational spectra. In addition, the intensity of the NO ion signal from energetic materials is proportional to the number of nitramine functional groups in the molecule. Based upon experimental observations and theoretical calculations of the potential energy surface for these systems, we suggest that energetic materials dissociate from ground electronic states after internal conversion from their first excited states, and model systems dissociate from their first excited states. In both cases a nitro-nitrite isomerization is suggested to be part of the decomposition mechanism. Parent ions of dimethylnitramine and nitropyrrolidine are observed in femtosecond experiments. All the other molecules generate NO as a decomposition product even in the femtosecond time regime. The dynamics of the formation of the NO product is faster than 180 fs, which is equivalent to the time duration of our laser pulse. © *2007 American Institute of Physics*. [DOI: 10.1063/1.2787587]

I. INTRODUCTION

Nitramine energetic materials, such as RDX (1,3,5-trinitro-1,3,5-triazacyclohexane), HMX (1,3,5,7-tetranitro-1,3,5,7-tetraazacyclooctane), and CL-20 (2,4,6,8,10,12-hexanitro-2,4,6,8,10,12-hexaazaisowurtzitane), have broad application as explosives and fuels due to their high energy content and high density. Except for the number of nitramine functional groups, these materials have similar structures which are shown in Fig. 1. As older and simpler nitramine energetic materials, RDX and HMX have been intensively investigated both theoretically and experimentally over the past decades.[1–8] These studies involve decomposition of RDX and HMX from both ground and excited electronic states, either in the condensed phase or in the gas phase. Studies of condensed phase energetic materials help one to understand how shock waves and impact can initiate the rapid exothermic chemical reactions that lead to detonation in explosive solids. On the other hand, studies of gas phase energetic materials reveal the properties and reactions of energetic materials at a molecular level, and determine the decomposition mechanism and dynamics as a function of electronic and vibrational state excitations.

Although many experimental and theoretical advances have occurred in understanding the initiation of the chemistry of energetic materials, the mechanisms of the decomposition of nitramines still remain uncertain. The following three initial steps in the decomposition of RDX and HMX from their ground electronic states have been proposed: (1) N–N bond fission to generate the NO_2 molecule;[9] (2) formation of a five-membered ring (OHCNN) to generate a HONO intermediate which then decomposes to NO and OH;[10,11] and (3) concerted symmetric ring opening to form three CH_2NNO_2 radicals.[12] Electronic excitation has been experimentally proven to play an important role in the initiation process of the detonation of energetic materials.[13–22] In order to understand the decomposition of gas phase energetic materials from their excited states, we have done several useful and informative experiments to reveal the initial steps in the dissociation of RDX and HMX from their first excited electronic states.[23–25] Results show that the NO molecule is a major decomposition product, while NO_2 and HONO have been ruled out as potential intermediates of the initial NO product. Two possible mechanisms for generation of the NO product are suggested: (1) N–N bond fission of the unstable nitrosamine intermediate [$(CH_2NNO_2)_2CH_2NNO$ or $(CH_2NNO_2)_3CH_2NNO$], which occurs after an O atom loss from the RDX or HMX molecule; and (2) nitro-nitrite isomerization of the RDX or HMX molecule with subsequent release of NO.

As a new and polycyclic energetic nitramine, CL-20 is expected to replace RDX and HMX in many applications

---

[a] Electronic mail: erb@lamar.colostate.edu

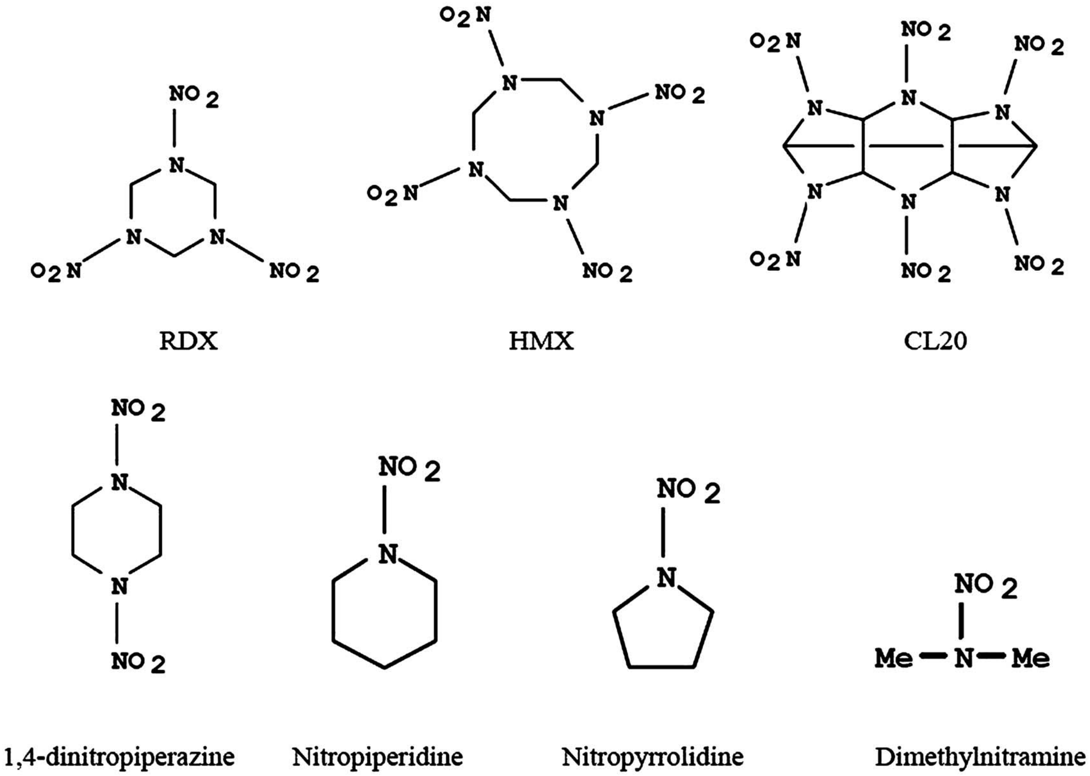

FIG. 1. Chemical structures of nitramine energetic materials (RDX, HMX, and CL-20) and model systems [dinitropiperazine, nitropiperidine, nitropyrrolidine, and dimethylnitramine (DMNA)].

due to its superior explosive performance. Although some theoretical studies[26,27] of CL-20 have been pursued since it was synthesized for the first time in 1998,[28] only a few experimental studies have been done on the decomposition of this energetic material.[29] Theoretical investigations show that CL-20 has similar decomposition mechanisms in its ground electronic state to that for RDX and HMX.[30]

Model systems, including 1,4-dinitropiperazine, nitropiperidine, nitropyrrolidine, and dimethylnitramine (DMNA), have similar molecular structure to the above energetic materials (shown in Fig. 1); however, they are unable to be used as fuels and explosives. In order to elucidate the difference between the energetic materials and model systems, we have experimentally and theoretically investigated the decomposition mechanisms and dynamics of both energetic materials and model systems from their excited electronic states. In this work, both nanosecond mass resolved excitation spectroscopy (MRES) and femtosecond pump-probe spectroscopy in the UV spectral region are employed to investigate the mechanisms and dynamics of the electronically excited photodissociation of CL-20 and the model systems. The only difference between the CL-20 and RDX and HMX experimental results is its more intense NO ion signal; thus, the decomposition behavior of CL-20 from its excited electronic state is the same as that found for RDX and HMX.[24,25] In the nanosecond MRES experiments, the dominant decomposition product for both the energetic materials and model systems is the NO molecule. Therefore we focus on the comparison between energetic materials and model systems mainly based on the NO molecule elimination channel. The NO molecule from decomposition of energetic materials displays different rotational and vibrational spectral properties than those of the model systems. Potential energy surface calculations on RDX and various model systems using second-order Møller-Plesset (MP2) and restricted single-excitation configuration interaction (RCIS) algorithms suggest that nitramine energetic materials dissociate from their ground electronic state with highly excited vibrational levels after an internal conversion from their first excited electronic state, while model systems dissociate from their first excited electronic states. In both cases, a nitro-nitrite isomerization is part of the decomposition mechanism. Parent ions of dimethylnitramine and nitropyrrolidine are observed in femtosecond experiments. All of the other molecules generate NO as a decomposition product even in the femtosecond time regime. The dynamics of the production of the NO molecule is within the time duration of our femtosecond laser pulse (180 fs).

II. EXPERIMENTAL PROCEDURES

Detailed experimental procedures for both nanosecond MRES and femtosecond pump-probe spectroscopy have been described in our previous publications.[23–25] Only the main components of the apparatus and some changes that have been made in this experiment will be briefly reviewed in this section. The experimental setup consists of laser systems with both nanosecond and femtosecond time duration, a supersonic jet expansion nozzle with a laser desorption attachment, and a time of flight mass spectrometer. The intact, gas phase, and isolated nitramine energetic materials are produced through a combination of matrix assisted laser desorption (MALD) and supersonic jet expansion. Due to the low vapor pressure of 1,4-dinitropiperazine, it has been placed into gas phase using the MALD technique too. The nozzle employed for the sample beam generation is constructed from a Jordan Co. pulsed valve and a laser desorption attachment.[31,32] The laser desorption head is attached to the front of the pulsed valve and has been described in detail in Ref. 24. In our previous experiments, a solution of equimolar amounts of sample and matrix (R6G dye) in acetone is uniformly sprayed on an Al_2O_3 coated drum.[33–36] In these experiments, we prepare all the sample drums for matrix desorption by wrapping a piece of porous filter paper around a clean aluminum drum rather than oxidizing a drum electrochemically for two reasons: (1) the procedure for preparing an Al_2O_3 coated drum is time consuming and removal of residual solution from the coating process, which produces interfering ion signals, is difficult; and (2) we find that a piece of porous filter paper as the deposition substrate has a similar behavior to that of the Al_2O_3 coating with regard to gas phase sample generation. The dried drum is then placed in the laser ablation head/nozzle assembly and put into a vacuum chamber. Nitramine molecules are desorbed from the drum by laser ablation at 532 nm, entrained in the flow of helium carrier gas through a 2 by 60 mm channel in the ablation head, and expanded into the vacuum chamber.[37,38] Model systems, other than 1,4-dinitropiperazine, are heated to about 350 K in a glass vial outside the nozzle and brought into the molecular beam by helium carrier gas with a varying pressure according to the vapor pressure of the samples.

In addition to the 532 nm ablation laser, one or two other lasers are required to photoexcite the energetic materials and model systems in the molecular beam and then detect the photodissociated products (NO in this case). For nanosecond MRES experiments, a single pump-probe laser is needed at 226–258 nm to both initiate dissociation of nitramine molecules and detect NO $[A(\mathrm{v}'=0)\leftarrow X(\mathrm{v}''=0-3)$ and $I\leftarrow A$ transitions$]$ through time of flight mass spectrometry (TOFMS). The proper UV laser wavelengths for this process are generated by a dye laser, pumped by the second harmonic (532 nm) of a Nd:yttrium aluminum garnet laser's fundamental output (1.064 μm), in conjunction with a wavelength extension system. For femtosecond pump-probe experiments, a single laser beam at 226 nm is equally split into pump and probe beams. The sample molecules are excited by the pump beam and dissociate according to their photodissociation dynamics. Photodissociation products are further ionized by the delayed probe beam and detected via the TOFMS. By delaying the probe beam with respect to the pump beam, product appearance times can be determined. The femtosecond laser light is generated by a femtosecond laser system consisting of a self-mode-locked Ti:sapphire oscillator (KM Labs), a home-made ring cavity Ti:sapphire amplifier, and a commercial traveling optical parametric amplifier of super fluorescence (Light Conversion) system. Pulse duration of the UV laser pulse has been measured to be 180 fs using a self-diffraction autocorrelator and off-resonance two-photon absorption of the furan molecule.[39]

The experiment is run at a repetition rate of 10 Hz. The timing sequence for the pulsed nozzle and the ablation laser is controlled by a time delay generator (SRS DG535). Ion signals are detected by a microchannel plate detector. Signals are recorded and processed on a personal computer using an ADC card (Analog Devices RTI-800) and a box car averager (SRS SR 250). For femtosecond pump-probe experiments, the delay time between the pump and probe beam is controlled by a microtranslation stage (Thorlabs: LNR50SEK1) for which a step size of 13 fs has been used. Each point on the pump-probe transient intensity curve corresponds to an average intensity resulting from 100 laser shots.

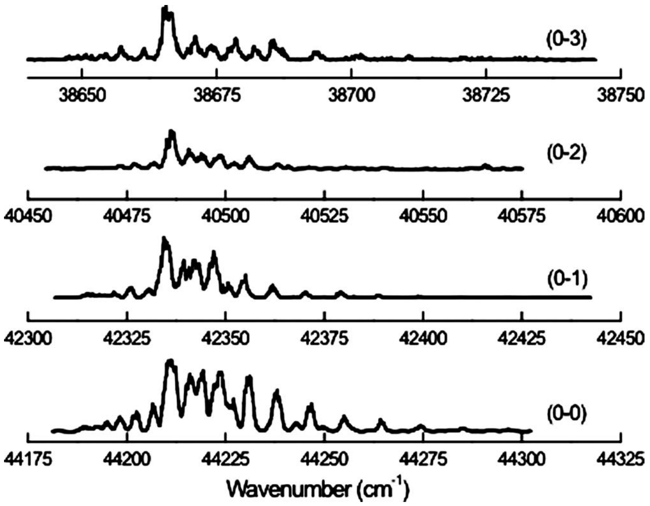

FIG. 2. 1-color MRES of the $A^2\Sigma(\mathrm{v}'=0)\leftarrow X^2\Pi(\mathrm{v}''=0,1,2,3)$ transitions of NO from CL-20.

III. CALCULATIONAL PROCEDURES

Potential energy and geometry calculations have been performed for RDX, nitropyrrolidine, and nitropiperidine with the Gaussian 98 program. The optimization of ground state geometries, and ground (S_0) transition state structures, as well as frequency calculations have been performed at a MP2/6-31G* level of theory. The optimizations of the first excited state geometries and excited (S_1) transition state structures, as well as frequency calculations, have been computed at a RCIS/6-31+G level of theory.

IV. RESULTS

Analysis of four vibronic transitions, $A^2\Sigma(\mathrm{v}'=0)\leftarrow X^2\Pi(\mathrm{v}''=0,1,2,3)$, of the NO molecule observed from nanosecond photodissociation of CL-20 excited to its first excited electronic state, by 226–258 nm UV laser light, shows similar results to the NO molecule observed from RDX and HMX (Fig. 2). The four spectra in Fig. 2 have similar rotational structure but have varying vibrational intensity for each vibronic band. As was shown for HMX and RDX[23,24] the most intense feature in each spectrum of NO from CL-20 corresponds to the $(Q_{11}+P_{12})$ band head while the less intense features within each spectrum correspond to rotational transitions.[40,41] Although the MALD technique is a

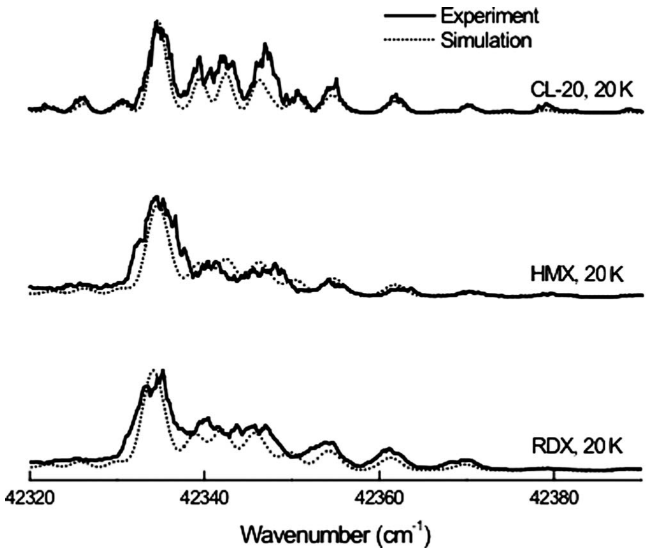

FIG. 3. Comparison of the 1-color MRES of the $A^2\Sigma(v'=0)\leftarrow X^2\Pi(v''=1)$ transition of NO from CL-20, HMX, and RDX.

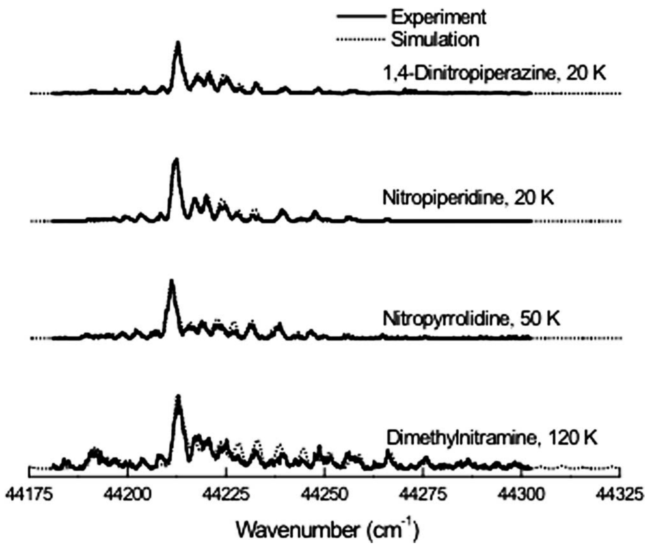

FIG. 4. 1-color MRES of the $A^2\Sigma(v'=0)\leftarrow X^2\Pi(v''=0)$ transition of NO from nitramine model systems.

good method to place easily fragmented, fragile molecules in the gas phase without fragmentation, great efforts are taken in our previous and present works to ensure that HMX, RDX, or CL-20 are not fragmented in the ablation process.[23,25] Three different methods have been employed to explore this issue: comparison of NO velocity distributions from the nozzle; determination of arrival time for the NO signal intensity as a function of nozzle/pump laser timing; and NO rotational and vibrational temperature determinations as a function of source of NO. These methods demonstrate that NO from HMX, RDX, and CL-20 is generated at the decomposition/ionization region of the TOFMS rather than in the ablation nozzle.

Figure 3 illustrates the $A\leftarrow X$ (0-1) transition spectra with simulations of the initial decomposition product, the NO molecule, of RDX, HMX, and CL-20. Comparisons of the three spectra confirm that the NO molecule from the decomposition of CL-20, HMX, and RDX has very similar rotational temperature (20 K) for the (0-1) vibronic transition. In addition, the observation of similar transition bands demonstrates that the NO molecule from the decomposition of CL-20 has about the same vibrational temperature ($\sim$1800 K) as that for RDX and HMX.[23,24] Thus we conclude that the NO molecule is an initial product of the electronically excited decomposition of the three energetic materials (RDX, HMX, and CL-20), the NO product is rotationally cold (20 K) and vibrationally hot (1800 K), and the UV photodecomposition of CL-20 experiences the same decomposition mechanism as that of RDX and HMX.

In efforts to improve our understanding of the excited state decomposition mechanisms of HMX, RDX, and CL-20, a number of model systems are explored. Although the NO molecule is still the only observed product of nanosecond UV photodecomposition of all the model systems from their excited electronic states, the global rotational and vibrational spectral distributions of the NO molecule generated in these processes are not only different from those of the energetic materials, but also from each other. Figure 4 presents the MRES spectra with simulations of the $A\leftarrow X$ (0-0) transition of the NO decomposition product for these model systems. Rotational temperatures of the NO product from 1,4-dinitropiperazine, nitropiperidine, dimethynitramine, and nitropyrrolidine are 20, 20, 120, and 50 K, respectively. NO from dimethylnitramine and nitropyrrolidine is rotationally hotter than NO from nitropiperidine and 1,4-dinitropiperazine suggesting the model systems which are more similar in structure to RDX, nitropiperidine, and dinitropiperazine could possibly follow similar decomposition routes to those of the energetic materials. Yet the comparisons shown in Fig. 5 suggest the model systems behave differently. The $A\leftarrow X$ (0-1) transitions of NO from model systems yield much hotter rotational temperatures (75, 700, and 100 K for 1,4-dinitropiperazine, nitropiperidine, and nitropyrrolidine, respectively) than those from the energetic materials. Calculational results in the following discussion will

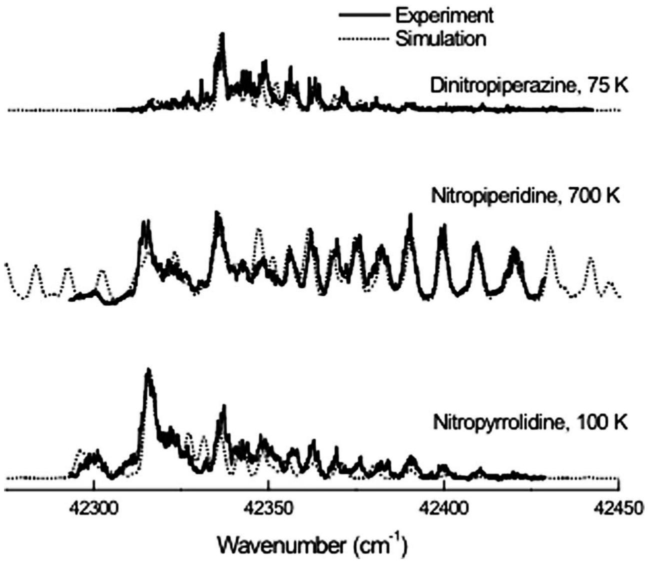

FIG. 5. 1-color MRES of the $A^2\Sigma(v'=0)\leftarrow X^2\Pi(v''=1)$ transition of the NO molecule from the nitramine model systems.

TABLE I. Rotational temperatures for the $A^2\Sigma\ (\mathrm{v}'=0) \leftarrow X^2\Pi\ (\mathrm{v}''=0,1,2,3)$ transitions of the NO product from nanosecond UV decomposition of energetic materials and model systems.

Sample	Rotational temperature $A \leftarrow X$ (0-0)	Rotational temperature $A \leftarrow X$ (0-1)	Rotational temperature $A \leftarrow X$ (0-2)	Rotational temperature $A \leftarrow X$ (0-3)
CL-20	20 K	20 K	20 K	20 K
HMX	20 K	20 K	20 K	20 K
RDX	20 K	20 K	20 K	20 K
Dinitropiperazine	20 K	75 K	⋯	⋯
Nitropiperidine	20 K	700 K	⋯	⋯
Nitropyrrolidine	50 K	100 K	⋯	⋯
Dimethylnitramine	120 K	⋯	⋯	⋯

yield insight into these seemingly inconsistent results. Table I gives rotational temperatures for each populated vibrational level of the NO product from both energetic materials and model systems. NO from energetic materials (RDX, HMX, and CL-20) has its first four vibrational levels populated $[X^2\Pi(\mathrm{v}'=0,1,2,3)]$ $(T_{\mathrm{vib}}=1800\ \mathrm{K})$, whereas NO from model systems has fewer vibrational states populated, indicating a cooler vibrational temperature. NO from dinitropiperazine, nitropiperidine, and nitropyrrolidine have measured vibrational signals for $X^2\Pi\ (\mathrm{v}''=0,1)$, but NO from dimethylnitramine is only observed in its ground vibrational level $[X^2\Pi(\mathrm{v}''=0)]$. In brief summary, overall vibrational temperature of NO from model systems is much less than that of NO from energetic materials.

Maximum NO ion signal intensity for nanosecond UV decomposition of energetic materials and model systems, and results for femtosecond UV decomposition of these materials are listed in Table II. The relative concentration of RDX, HMX, and CL-20 is assumed to be the same in the ionization region due to the fact that equal molar amounts of each material are placed on the sample drum. Comparing the ion signal intensity of NO from each energetic material yields an approximate ratio of 3:4:6 for RDX:HMX:CL-20, corresponding to the number of nitramine moieties within each material. This signal intensity suggests that energetic materials decompose via the same mechanism in which each nitramine group yields a NO molecule. On the femtosecond time scale, parent ions of DMNA and nitropyrrolidine are observed if 226 nm fs light pulses are employed to photodissociate these nitramine systems (as shown in Fig. 6). Table II illustrates that all other systems explored in the femtosecond time regime yield the NO product.

TABLE II. Comparison of maximum NO ion signal intensity (nanosecond) and photodissociation products (femtosecond) for the energetic materials and model systems.

Sample	NO$^+$ intensity (ns)	Femtosecond result
CL-20	3.7 V	NO product decomposes <180 fs
HMX	2.0 V	NO product decomposes <180 fs
RDX	1.5 V	NO product decomposes <180 fs
Dinitropiperazine	300 mV	NO product decomposes <180 fs
Nitropiperidine	255 mV	NO product decomposes <180 fs
Nitropyrrolidine	160 mV	Stable ion
Dimethylnitramine	150 mV	Stable ion

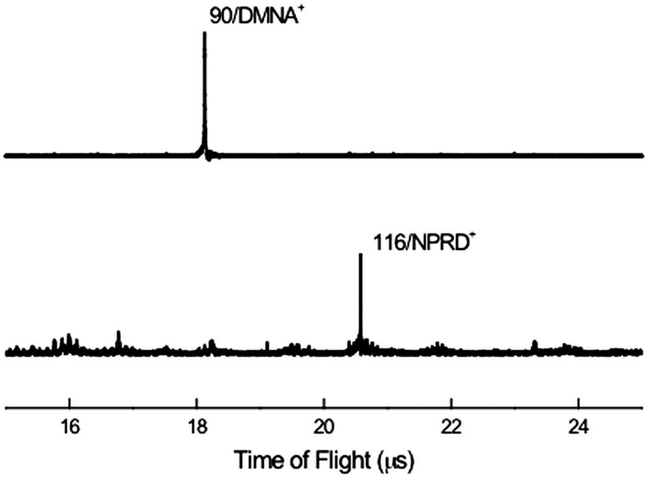

FIG. 6. Mass spectra of dimethylnitramine (upper) and nitropyrrolidine (lower) using 226 nm femtosecond excitation.

Figure 7 displays femtosecond pump-probe transients for the NO product from RDX (b) and CL-20 (c) at 226 nm. The NO molecule has a resonant single photon absorption for the $A^2\Sigma(\mathrm{v}'=0) \leftarrow X^2\Pi(\mathrm{v}''=0)$ transition at 226 nm. Both pump and probe beams have the same wavelength. As described in our previous report,[25] the gas phase energetic material is pumped to its first excited electronic state by the pump beam, it dissociates into products according to its corresponding mechanisms and dynamics, and its initial products are probed. The dynamics of the decomposition are measured via NO molecule appearance. If decomposition of the energetic materials is slower than the time duration of pump and probe beams (180 fs), an (exponential) onset of the NO ion signal will be observed as the relative delay time between pump and probe beams is scanned. If decomposition of the energetic materials is much faster than the pulse duration,

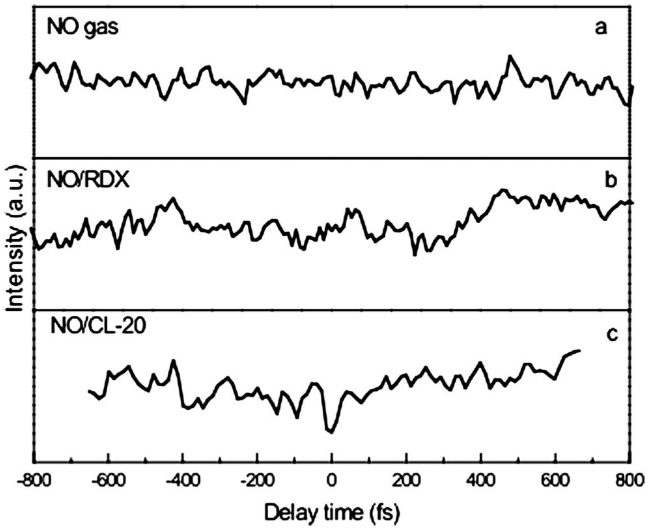

FIG. 7. Femtosecond pump-probe transients for the NO molecule from NO gas (a), and the photodissociation of RDX (b) and CL-20 (c) at 226 nm. The NO $A^2\Sigma(\mathrm{v}'=0) \leftarrow X^2\Pi(\mathrm{v}''=0)$ transition has a single-photon resonant absorption at 226 nm.

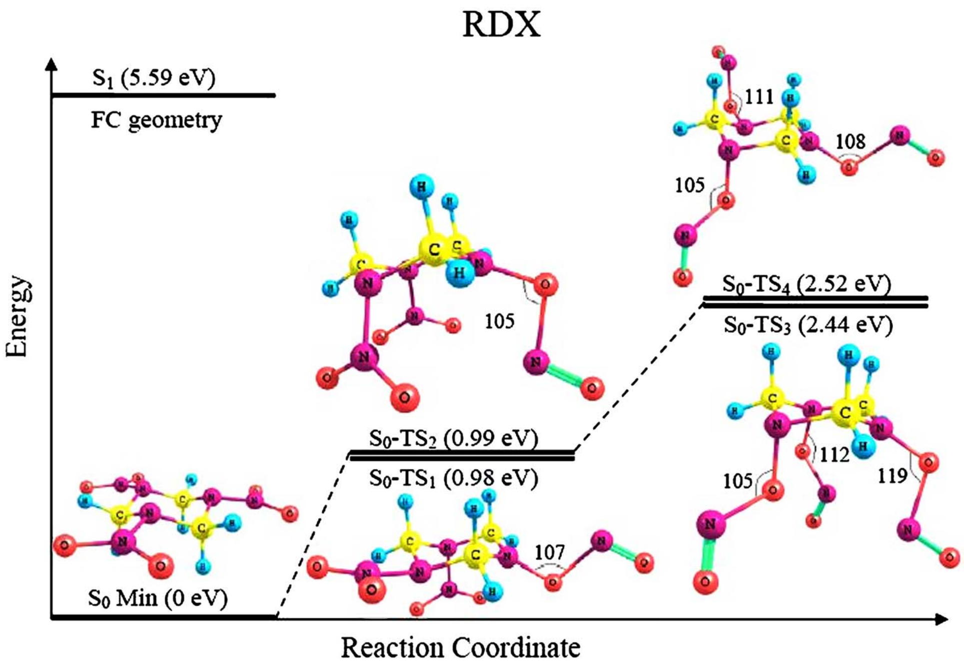

FIG. 8. (Color online) Potential energies and structures of the transition states of RDX in its ground electronic states. Energies are in eV.

NO product will be excited by the pump beam in addition to the probe beam, and the lifetime of the NO excited state, which is several hundred nanoseconds, will be detected by the probe beam, and the pump-probe transient for the NO product should be a flat horizontal line within a many picosecond time interval. As mentioned in Sec. II, both pump and probe beams are identical, either one could be pump or probe beam depending on the relative delay time between the two beams. Thus, identical behavior at both negative and positive delay times, rather than a sharp step at zero time will be observed in these pump-probe experiments. At low photon density (2.2×10^6 W/cm^2) used in these experiments, single femtosecond laser beam generates about 10 mV intensity of NO ion signal, and the total pump-probe ion signal is about 30 mV. The transients in Fig. 7 show a roughly steady NO ion signal from both RDX and CL-20, which is the same as NO gas, indicating the dynamics of energetic materials occur on a faster time scale than the time duration of our laser pulse. Similar results are found for nitropiperidine and 1,4-dinitropiperazine suggesting that these larger more representative model systems also have fast dissociation dynamics.

In order to understand better the experimental data, calculations of geometries, energies, transition state (TS) structures, and frequencies for both the ground (S_0) and excited (S_1) states have been performed for both energetic materials and model systems. Two possible decomposition mechanisms are calculationally explored in efforts to yield insight into the experimental findings. The first mechanism includes an excited state dissociation that follows a decomposition channel through an isomerization of the nitramine moieties. The second mechanism involves ground state dissociation after internal conversion from the excited state, in which the decomposition follows a path through the concerted nitro-nitrite isomerization of the nitramine moieties. These two reaction channels are chosen for approximation because the decomposition of energetic materials generates highly vibrationally excited NO molecules, but decomposition of model systems generates the NO product with high rotational temperatures. The calculated potential energy and optimized geometry diagrams of RDX, nitropiperidine, and nitropyrrolidine are illustrated in Figs. 8–10, respectively. The theoretical vertical excitation energies for RDX, nitropiperidine, and nitropyrrolidine are 5.59, 5.62, and 5.85 eV, respectively. For the ground electronic state, both nitropiperidine and nitropyrrolidine have an isomerization transition state (S_0-TS) with similar NONO moiety structures at an energy of ~1 eV; RDX has two single nitro-nitrite isomerization transition states (S_0-TS$_1$ and S_0-TS$_2$) at an energy of ~1 eV and two additional unique concerted nitro-nitrite isomerization states (S_0-TS$_3$, S_0-TS$_4$) at an energy 1.4 eV above the single nitro-nitrite isomerization states. The potential energy level for the final products (R+NO) is not plotted in the diagrams. The ∠NON bond angles of transition states are labeled in Figs. 8–10 for analysis of rotational distribution for NO product. The ∠NON bond angle for the ground transition state geometry of RDX, nitropyrrolidine, and nitropiperidine, is around 105°–110°, and the negative frequency or unstable normal mode of vibration is characterized by the out-of-plane bending of the ONCC moiety. This motion corresponds to a true nitro-nitrite isomerization. The excited transition state geometry (S_1-TS) of nitropyrrolidine shows a ∠NON bond angle of 31°, much smaller than that of the ground transition state (S_0-TS). In addition, its unstable normal mode of vibration relates to an asymmetric stretch of the ONO moiety. For the excited transition state (S_1-TS) of nitropiperidine, the ∠NON bond angle is about 110°. The unstable normal mode of vibration of this geometry is associated with the rotation of the terminal NO around the elongated ON bond. Optimization of the excited state geometry of RDX does not converge at the level of RCIS/6-31+G theory.

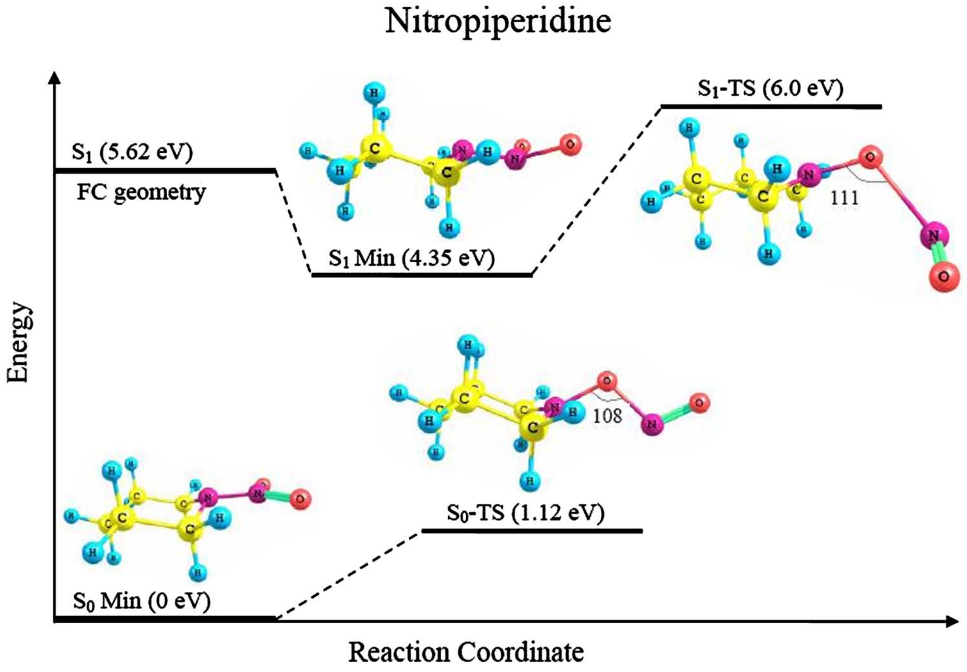

FIG. 9. (Color online) Potential energies and structures of the transition states of nitropiperidine in its ground and first excited electronic states. Energies are in eV.

V. DISCUSSION

In Sec. IV, we conclude that the NO molecule is an initial nanosecond UV decomposition product for both energetic materials and model systems of interest in this work; however, energetic materials present a rotationally cold and vibrationally hot NO molecule, while model systems give a rotationally hot yet vibrationally cold NO molecule. These results imply that energetic materials and model systems should experience different dissociation channels after UV laser excitation.

Calculations at the RCIS/6-31+G theory level show that vertical excitation energies of RDX (5.59 eV), nitropiperidine (5.62 eV), and nitropyrrolidine (5.85 eV) are very close to the energy of a single photon in the range of 226–258 nm (~5.5–5 eV), which has been used to photodissociate these materials. Additionally, the S_1 transition states of both nitropiperidine and nitropyrrolidine are similar in energy to the vertical excitation energy (~5.5 eV), therefore these molecules will not have enough energy within the electronically excited state after surmounting the S_1 transition state energy threshold to produce a highly vibrationally excited NO product. On the contrary, if we suppose that RDX undergoes an internal conversion from its excited electronic state to its ground electronic state, this process would yield sufficient extra vibrational energy (~5 eV) to surmount the concerted nitro-nitrite isomerization transition states (S_0-TS$_3$, S_0-TS$_4$ in Fig. 8), which have an energy of about 2.4 eV above the ground electronic state, and to generate NO product with

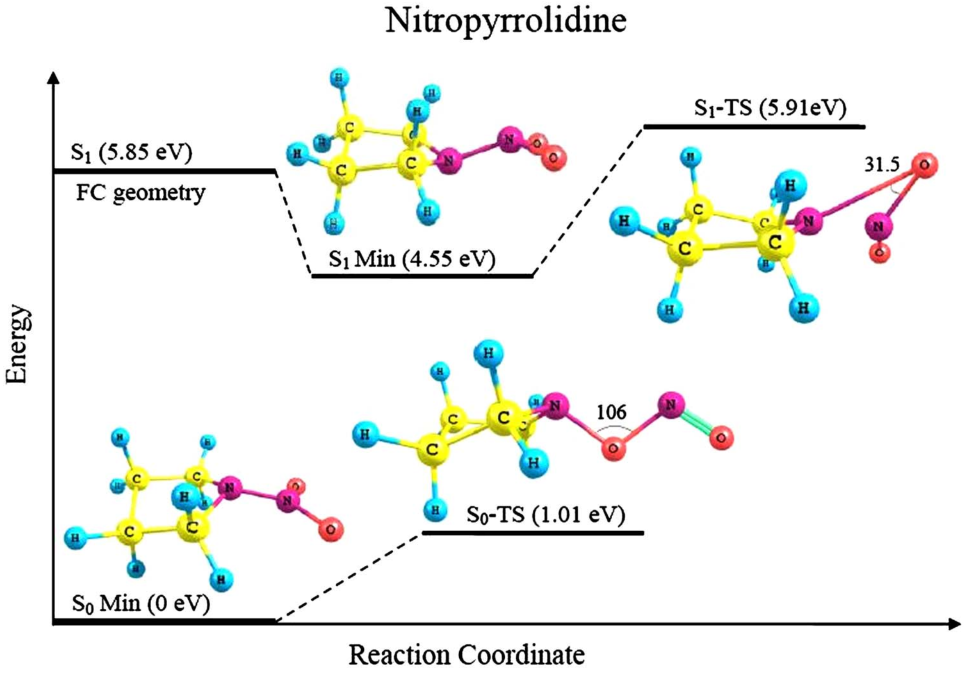

FIG. 10. (Color online) Potential energies and structures of the transition states of nitropyrrolidine in its ground and first excited electronic states. Energies are in eV.

high vibrational excitation. The suggestion of a specific nitro-nitrite isomerization transition state is supported both theoretically and experimentally: an (S_1/S_0) conical intersection has been recently reported for the NH_2NO_2 system that results in a nonadiabatic decomposition through nitro-nitrite isomerization from its excited electronic state;[42] and we have not observed NO_2 or OH in our experiments. Such a nitro-nitrite isomerization pathway is not directly accessible in the ground state because the presence of this conical intersection destroys the minimum energy path on the ground state surface. In addition, this suggested decomposition pathway for energetic materials should produce a concentration of NO molecule proportional to the number of the nitramine functional groups of each energetic material, in good agreement with our experimental observation of the ratio of NO ion signal intensity for RDX, HMX, and CL-20 close to 3:4:6. Compared to the decomposition of RDX, the UV decomposition of nitropiperidine and nitropyrrodine produce NO products with cooler vibrational temperature, which indicates that the model systems should decompose through their excited electronic states. In the model systems, a small amount of extra energy, above the excited transition state zero point level, may be available to excite the low frequency bending modes of the parent molecule (nitropiperidine and nitropyrrolidine), which could result in a NO product with a low vibrational temperature and a high rotational temperature.

The $\angle$NON bond angle of the transition state species, which forms during the nitro-nitrite isomerization process and shows large difference in different molecules, is an important parameter for determining the rotational excitation of the NO product from all the systems of interest because this bond angle determines how much torque the NO moiety should experience during the dynamical process of nitro-nitrite isomerization followed by NO elimination. The reaction coordinate (or nuclear coordinate) for nitro-nitrite isomerization is composed of NN bond elongation and NO bond formation. Therefore, the $\angle$NON bond angle is a reflection of the impulse (torque) to the NO moiety from the NN bond elongation. A smaller $\angle$NON bond angle will result in larger torque for the NO product, namely, higher rotational excitation of the NO molecule, which leads to a hot rotational distribution of NO. Conversely, a larger $\angle$NON bond angle will result in smaller or no torque for the NO product, which leads to cooler rotational temperature for NO. Thus, the difference in behavior of the rotational excitation of the NO product will be mainly influenced by $\angle$NON bond angle, not by $\angle$ONO bond angle, which has a similar value $(\sim 110^\circ - 120^\circ)$ for all systems and undergoes insignificant change during the nitro-nitrite isomerization. The $\angle$NON bond angles of the two concerted nitro-nitrite isomerization transition states of ground state RDX are around 110°, therefore the decomposition of RDX through these transition states should produce NO product with relatively cold rotational temperature. The four vibronic transition spectra of NO from RDX display low rotational temperatures (20 K), further confirming that RDX, as well as the other two energetic materials, should decompose through its ground electronic state after internal conversion from their excited electronic states. Due to similar TS structures and unstable normal modes of vibration, a decomposition mechanism through the ground TS for RDX, nitropiperidine, and nitropyrrolidine should yield similar NO molecule vibrational and rotational distributions for all four precursors. This is not found to be true experimentally, however, suggesting again that the energetic materials decompose through a different path than the model systems.

Nitropyrrolidine has a much smaller S_1-TS $\angle$NON bond angle than that of its S_0-TS, as shown in Fig. 10. Therefore, if nitropyrrolidine decomposes through its excited transition state, the bond angle, $\angle NON = 32^\circ$, would result in a hot NO rotational population. Experimentally, the (0-0) and (0-1) vibronic transitions of the NO product from nitropyrrolidine have rotational temperatures of 50 and 100 K, respectively, which are hotter than that found for the NO product from energetic materials. Additionally, the unstable normal mode of vibration of the S_1 transition state of nitropyrrolidine is associated with an asymmetric stretch of the ONO moiety, which leads to a real nitro-nitrite isomerization pathway for the decomposition of this model system. Based on the comparison between RDX and nitropyrrolidine, one expects that nitropyrrolidine should decompose through its excited electronic state via a nitro-nitrite isomerization mechanism.

As mentioned Sec. IV, the $\angle$NON bond angle of S_1-TS of nitropiperidine is about 110°, comparable to that of its ground transition state (S_0-TS). Therefore, even if nitropiperidine decomposes through its excited electronic state, an NO product with cold rotational distribution could be generated from the vibrationless excitation of the isomerization transition state. This is illustrated by the (0-0) vibronic transition of the NO product from this molecule, which displays a rotational temperature of 20 K, the same temperature as that from energetic materials. Moreover, frequency calculations show that the unstable normal mode of vibration of the S_1-TS geometry of nitropiperidine (unlike that for nitropyrrolidine) is associated with the rotation of NO terminal group around an elongated ON bond, which could result in a highly rotationally populated NO product. This can explain why the (0-1) vibronic transition of the NO product from this molecule has a 700 K rotational temperature, much hotter than its (0-0) transition and the (0-1) transition of NO product from nitropyrrolidine. According to the above analysis, decomposition mechanism through the nitro-nitrite isomerization excited transition state (S_1-TS) is in good agreement with experimental results for both nitropyrrolidine and nitropiperidine. The other two model systems, 1,4-dinitropiperazine and dimethylnitramine, have similar decomposition behavior to that of nitropiperidine and nitropyrrodine, thus we conjecture that all the model systems decompose through the same excited electronic state pathway to generate NO product with hot rotational and cold vibrational temperatures. NO from DMNA at 226 nm excitation is vibrationally cold, only the (0-0) transition is observed, and rotationally hot (120 K). This hot rotational distribution and cold vibrational distribution of NO is consistent with a nitro-nitrite isomerization but not a NO_2 elimination mechanism. Note that NO from NO_2 gas (excited at 226 nm) is also rotationally hot for the (0-0) transition but it is vibrationally hotter than NO from dimethylnitramine because both

(0-0) and (0-1) transitions are observed.[43] At 236 and 248 nm excitations, (0-1) or (0-2) transition of the NO product has not been observed from dimethylnitramine. This is in good agreement with Ref. 44, where NO product was not detected, and NO_2 and OH were proposed to be the major products for decomposition of dimethylnitramine at 248 nm. The proposed nitro-nitrite decomposition mechanism of dimethylnitramine following 226 nm photoexcitation differs from that found at both 248 and 266 nm, which essentially results in NO_2 elimination as the initial decomposition pathway.[44,45] A possible reason for this different mechanistic behavior as a function of excitation energy is that with 5.5 eV (226 nm) excitation dimethylnitramine can surmount an energy barrier for nitro-nitrite isomerization in the excited state, whereas at both 248 nm (5.0 eV) and 266 nm (4.7 eV) dimethylnitramine cannot surmount this isomerization barrier. Further calculations at the complete active space self-consistent field (CASSCF) level of theory are being pursued to explore this particular model system behavior.

Only parent ions of DMNA and nitropyrrolidine are observed through femtosecond UV multiphoton ionization, indicating that multiphoton ionization of these parent molecules within the femtosecond temporal regime overwhelms decomposition through their excited electronic state. All other systems generate NO as a decomposition product and the dynamics of the decomposition of these other systems are faster than 180 fs. We are pursuing theoretical calculations to explore the experimental results on the femtosecond time regime, but high theory levels are required for a more quantitative understanding of these dynamics.

VI. CONCLUSIONS

Electronically excited photodissociaiton of nitramine energetic materials (RDX, HMX, and CL-20) and models systems (1,4-dinitropiperazine, nitropiperidine, nitropyrrolidine, and dimethylnitramine) has been investigated via both nanosecond MRES and femtosecond pump-probe techniques. The NO molecule is a dominant product of both the energetic materials and model systems. The NO molecule from energetic materials displays cold rotational and hot vibrational spectral structures, while the NO molecule from the model systems shows relatively hot rotational, but cold vibrational temperatures. Experimental observations and theoretical calculations suggest that energetic materials dissociate from their ground electronic states with high vibrational excitation after an internal conversion from their first excited states, and model systems dissociate directly from their first excited states. These processes yield NO product with different rotational and vibrational temperatures for energetic and model precursors. In both cases, nitro-nitrite isomerization is suggested to be part of the decomposition mechanism. Parent ions of dimethylnitramine and nitropyrrodine are observed in femtosecond experiments. All of the other systems generate the NO molecule as a product even in the femtosecond time regime. The dynamics of this decomposition is faster than 180 fs, which is equivalent to the time duration of our laser pulse.

ACKNOWLEDGMENTS

This research was supported by grants from ARO and DOD DURIP.

[1] F. J. Owens and J. Sharma, J. Appl. Phys. **51**, 1494 (1980).
[2] S. Bulusu, D. I. Weinstein, J. R. Autera, and R. W. Velicky, J. Phys. Chem. **90**, 4121 (1986).
[3] J. J. Dick, R. N. Mulford, W. J. Spencer, D. R. Pettit, E. Garcia, and D. C. Shaw, J. Appl. Phys. **70**, 3572 (1991).
[4] J. C. Oxley, A. B. Kooh, R. Szekeres, and W. Zheng, J. Phys. Chem. **98**, 7004 (1994).
[5] W. Fickett and W. C. Davis, *Detonation* (University of California Press, Berkeley, 1979).
[6] F. H. Ree, J. Chem. Phys. **81**, 1251 (1984).
[7] Y. Kohno, K. Ueda, and A. Imamura, J. Phys. Chem. **100**, 4701 (1996).
[8] D. C. Sorescu, B. M. Rice, and D. L. Thompson, J. Phys. Chem. B **102**, 6692 (1998).
[9] C. Capellos, S. Lee, S. Bulusu, and L. Gams, *Advances in Chemical Reaction Dynamics* (Reidel, Dordrecht, 1986).
[10] H. Zuckermann, G. D. Greenblatt, and Y. Haas, J. Phys. Chem. **91**, 5159 (1987).
[11] C. Capellos, P. Papagiannakopoulos, and Y.-L. Liang, Chem. Phys. Lett. **164**, 533 (1989).
[12] X. S. Zhao, E. J. Hintsa, and Y. T. Lee, J. Chem. Phys. **88**, 801 (1988).
[13] H. M. Windawi, S. P. Varma, C. B. Cooper, and F. Williams, J. Appl. Phys. **47**, 3418 (1976).
[14] J. Schanda, B. Baron, and F. Williams, Acta Tech. Acad. Sci. Hung. **80**, 185 (1975).
[15] J. Schanda, B. Baron, and F. Williams, J. Lumin. **9**, 338 (1974).
[16] S. P. Varma and F. Williams, J. Chem. Phys. **59**, 912 (1973).
[17] R. B. Hall and F. Williams, J. Chem. Phys. **58**, 1036 (1973).
[18] F. Williams, Adv. Chem. Phys. **21**, 289 (1971).
[19] A. N. Dremin, V. Y. Klimenko, O. N. Davidoua, and T. A. Zolodeva, Proceedings of the 9th Symposium On Detonation, Portland Oegon, 1989, p. 319.
[20] J. Sharma, B. C. Beard, and M. Chaykovsky, J. Phys. Chem. **95**, 1209 (1991).
[21] J. Sharma, J. W. Forbes, C. S. Coffey, and T. P. Liddiard, J. Phys. Chem. **91**, 5139 (1987).
[22] J. Sharma, APS Topical Meeting on Shocks in Energetic Materials, Williamsburg VA, 1991.
[23] H. S. Im and E. R. Bernstein, J. Chem. Phys. **113**, 7911 (2000).
[24] Y. Q. Guo, M. Greenfield, and E. R. Bernstein, J. Chem. Phys. **122**, 244310 (2005).
[25] M. Greenfield, Y. Q. Guo, and E. R. Bernstein, Chem. Phys. Lett. **430**, 277 (2006).
[26] B. M. Rice and J. Hare, Thermochim. Acta **384**, 377 (2002).
[27] G. Zhou, J. Wang, W.-D. He, N.-B. Wong, A. Tian, and W.-K. Li, J. Mol. Struct.: THEOCHEM **273**, 589 (2002).
[28] A. T. Nielsen, A. P. Chafin, S. L. Christian, D. W. Moore, M. P. Nadler, R. A. Nissan, D. J. Vanderah, R. D. Gilardi, C. F. George, and J. L. Flippen-Anderson, Tetrahedron **54**, 11793 (1998).
[29] J. Cabalo and R. Sausa, Appl. Opt. **44**, 1084 (2005).
[30] S. Okovytyy, Y. Kholod, M. Qasim, H. Fredrickson, and J. Leszczynski, J. Phys. Chem. A **109**, 2964 (2005).
[31] M. Foltin, G. J. Stueber, and E. R. Bernstein, J. Chem. Phys. **111**, 9577 (1999).
[32] M. Foltin, G. J. Stueber, and E. R. Bernstein, J. Chem. Phys. **114**, 8971 (2001).
[33] G. P. Wirtz, S. Brown, and W. M. Kriven, Mater. Manuf. Processes **6**, 87 (1991).
[34] P. Kurze, W. Krysmann, J. Schreckenbach, T. Schwarz, and K. Rabending, Cryst. Res. Technol. **22**, 53 (1987).
[35] W. Krysmann, P. Kurze, K.-H. Dittrich, and H. G. Schneider, Cryst. Res. Technol. **19**, 973 (1984).
[36] K.-H. Dittrich, W. Krysmann, P. Kurze, and H. G. Schneider, Cryst. Res. Technol. **19**, 93 (1984).
[37] P. Carcabal, R. T. Kroemer, L. C. Snoek, J. P. Simons, J. M. Bakker, I. Compagnon, G. Meijer, and G. V. Helden, Phys. Chem. Chem. Phys. **6**, 4546 (2004).
[38] L. C. Snoek, T. V. Mourik, and J. P. Simons, Mol. Phys. **101**, 1239 (2003).
[39] R. Trebino, *Frequency-Resolved Optical Gating: The Measurement of*

Ultrafast Laser Pulses (Kluwer Academic, Boston, 2000).
[40] M. Hippler and J. Pfab, Chem. Phys. Lett. **243**, 500 (1995).
[41] G. Herzberg, *Spectra of Diatomic Molecules* (Van Nostrand, New York, 1950).
[42] J. Soto, J. F. Arenas, J. C. Otero, and D. Pelaez, J. Phys. Chem. A **110**, 8221 (2006).
[43] H. S. Im and E. R. Bernstein, J. Phys. Chem. A **106**, 7565 (2002).
[44] M. J. McQuaid, A. W. Miziolek, R. C. Sausa, and C. N. Merrow, J. Phys. Chem. **95**, 2713 (1991).
[45] J. C. Mialocq and J. C. Stephenson, Chem. Phys. Lett. **123**, 390 (1986).